

Spatial relationships between the pharmacophores of endomorphin-2: a comparative study of stereoisomers

Short Communication

Balázs Leitgeb*

*Institute of Biophysics, Biological Research Centre,
Hungarian Academy of Sciences, H-6726 Szeged, Hungary*

Received 19 April 2012; Accepted 31 July 2012

Abstract: The spatial relationships between the pharmacophore elements were investigated in the case of four different stereoisomeric forms of opioid tetrapeptide, endomorphin-2, taking into account the L-D and *cis-trans* isomerisms. On the basis of distances and angles measured between the pharmacophoric points, a comparative analysis of conformational distributions was performed, applying a variety of distance-angle maps. The results obtained by this theoretical study indicated that the stereoisomers of endomorphin-2 could be distinguished from one another, based on the comparative analysis of distance-angle maps. Nevertheless, it could be concluded that this method proved to be suitable to examine the effects of L-D and *cis-trans* isomerisms on the spatial relationships of the pharmacophores of tetrapeptide.

Keywords: *Endomorphin • Pharmacophore • Conformational analysis • L-D isomerism • Cis-trans isomerism*
© Versita Sp. z o.o.

1. Introduction

Endomorphin-2 (EM2, H-Tyr-Pro-Phe-Phe-NH₂) is an opioid tetrapeptide possessing high activity and selectivity toward the μ -opioid receptor [1]. The three-dimensional (3D) structural features of endomorphins (EMs) and their analogs have been studied by means of various experimental and theoretical methods [2]. In our previous structural investigations, detailed conformational analyses were carried out on the EMs applying different computational methods, in order to identify their characteristic structural and conformational properties [3-6]. These theoretical studies led to several valuable observations concerning the 3D structural features of these tetrapeptides, as well as regarding their possible biologically active form. In a recent study, a comparative conformational analysis was performed for all the stereoisomeric forms of EM2, taking into consideration both the L-D and *cis-trans* isomerisms [7]. For the thirty-two stereoisomers of tetrapeptide, a comprehensive structural characterization was carried out, and their typical features were determined, with regard to the Φ - Ψ conformational distributions and the rotamer states, as

well as to the secondary structural elements and the intramolecular interactions. Based on the results derived from these theoretical calculations, it was concluded that both conformational similarities and dissimilarities could be observed between the stereoisomeric forms of EM2, and it was clarified how their 3D structural features differed from one another.

The data obtained by earlier studies indicated that four groups could be considered as pharmacophore elements for the EMs, as follows: (1) the N-terminal amino group; (2) the aromatic side-chain of the Tyr¹ amino acid; (3) the aromatic side-chain of the Trp³/Phe³ residue; (4) the aromatic side-chain of the Phe⁴ amino acid [2]. Thus, the relative spatial arrangement of these putative pharmacophores seems to be important in the formation of the biologically active form of these tetrapeptides. Previously, a novel approach (CSP, Conformationally Sampled Pharmacophore) was applied for nonpeptidic and peptidic ligands showing selectivity toward the δ -opioid receptor [8-10]. This method was developed based on the characterization of all possible combinations of distances and angles measured between the pharmacophore elements of

* E-mail: leitgeb@brc.hu

ligands, as well as on the comparative analyses of various conformational distributions. The results derived from these computational studies led to the conclusion that the CSP approach proved to be suitable for these molecules, to differentiate the agonists from the antagonists.

In the present theoretical study, the spatial relationships between the pharmacophores of EM2 were characterized by a variety of distance-angle maps, applying distances and angles measured between the pharmacophoric points. This structural investigation was performed on four different stereoisomers of the tetrapeptide, considering the L-D and *cis-trans* isomerisms, and the various conformational distributions regarding the stereoisomeric forms were compared to one another. The aims of this work were to examine the effects of both aforementioned isomerisms on the spatial relationships with regard to the pharmacophores of EM2, as well as to determine whether the CSP method can be applied to distinguish the stereoisomers of tetrapeptide from one another.

2. Experimental procedure

To explore the conformational spaces of peptides, simulated annealing (SA) calculations were performed with the AMBER 9 program [11], applying the AMBER 99SB force field [12] and the Generalized Born implicit solvent model [13-15], using no cutoff for the nonbonded interactions. After an initial energy-minimization, the geometrically optimized structures were heated to 1000 K for 1000 fs, then equilibrated at 1000 K during 4000 fs, and finally cooled from 1000 K to 50 K for 10000 fs. In the cooling stage, a near-exponential protocol was applied, consisting of the following three linear phases: (1) from 1000 K to 500 K during 1000 fs; (2) from 500 K to 200 K during 2000 fs; (3) from 200 K to 50 K during 7000 fs. The SA cycle - involving the heating, equilibration and cooling stages - was carried out 1000 times, thus for each peptide, 1000 conformers were obtained by the SA calculations. Thereafter, a final energy-minimization was performed in the case of all structures derived from the SA simulations. For this geometry optimization, the steepest descent method was used during the first 100 steps, and subsequently, the conjugated gradient algorithm was applied, with a gradient convergence criterion of 0.001 kcal mol⁻¹ Å⁻¹, and with the maximum number of iterations of 10000.

The aforementioned SA calculations were carried out on four different stereoisomeric forms of the parent peptide, as follows: (1) EM2 - containing L-amino acids - with *trans* Tyr¹-Pro² peptide bond (labeled as **S[1]**);

(2) *enanti*-EM2 - containing D-amino acids - with *trans* Tyr¹-Pro² peptide bond (labeled as **S[2]**); (3) EM2 with *cis* Tyr¹-Pro² peptide bond (labeled as **S[3]**); (4) *enanti*-EM2 with *cis* Tyr¹-Pro² peptide bond (labeled as **S[4]**).

3. Results and discussion

In order to characterize the conformational distributions, various distance-angle maps were produced, in which the distances and angles measured between the pharmacophore elements were represented. Taking into consideration the pharmacophore groups of EM2, the pharmacophoric points were defined as the N atom for the N-terminal amino (NH₃⁺) group, and as the centroids of the six-membered phenyl rings of aromatic side-chains for the Tyr¹, Phe³ and Phe⁴ residues. These points were labeled as **N** in the case of NH₃⁺ group, and **A**, **B** and **C** in the case of Tyr¹, Phe³ and Phe⁴ amino acids, respectively. Two different subgroups were distinguished with regard to the pharmacophore elements: the first subgroup included the **N**, **A** and **B** points, while the other one covered the **N**, **A** and **C** points. For both of them, three distances and three angles were defined and calculated, as follows: (1) for the first subgroup, the (**N-A**), (**N-B**) and (**A-B**) distances; and the (**N-A-B**), (**N-B-A**) and (**A-N-B**) angles; (see Fig. 1a) (2) for the second subgroup, the (**N-A**), (**N-C**) and (**A-C**) distances; and the (**N-A-C**), (**N-C-A**) and (**A-N-C**) angles (see Fig. 1b). Applying these geometric parameters, nine different types of distance-angle maps were constructed in the case of both subgroups, according to the nine possible combinations of distances and angles. On the basis of these plots, the ranges of distances were divided into 0.5 Å intervals, whereas the ranges of angles were divided into 5° intervals, resulting in various regions in the distance-angle maps. Then, the number of conformations was determined for all the regions, and conformational similarity indices (CS_{xx'}) [7,16,17] were calculated in order to compare the conformational distributions using the following equation:

$$CS_{xx'} = \frac{\sum_i (N_{xi} - \langle N_x \rangle)(N_{xi'} - \langle N_{x'} \rangle)}{\sqrt{\sum_i (N_{xi} - \langle N_x \rangle)^2 \sum_i (N_{xi'} - \langle N_{x'} \rangle)^2}}$$

where N_{xi} and $N_{xi'}$ are the numbers of conformations in the *i*th region of certain distance-angle maps for two different stereoisomers, respectively, whereas $\langle N_x \rangle$ and $\langle N_{x'} \rangle$ are the average numbers of conformations with regard to certain distance-angle maps of two stereoisomeric forms, respectively. The calculated CS_{xx'} indices were represented in 4×4 lower triangular matrices for each distance-angle pair, in accordance with the four different stereoisomers of tetrapeptide.

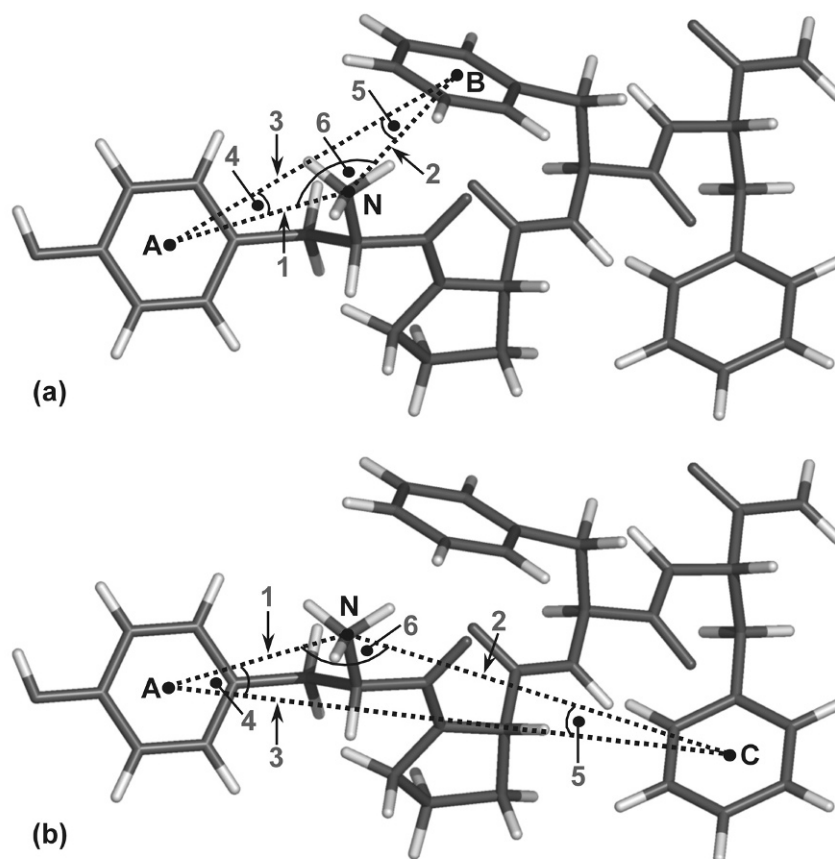


Figure 1. Distances and angles measured between the pharmacophoric points with regard to two subgroups of the pharmacophore elements. (a) For the first subgroup: (1) the (N-A), (2) the (N-B) and (3) the (A-B) distances; (4) the (N-A-B), (5) the (N-B-A) and (6) the (A-N-B) angles. (b) For the second subgroup: (1) the (N-A), (2) the (N-C) and (3) the (A-C) distances; (4) the (N-A-C), (5) the (N-C-A) and (6) the (A-N-C) angles.

The nine different types of distance-angle maps, concerning the first subgroup of pharmacophore elements, are illustrated in Figs. 2 and 3 for the **S[1]** and **S[2]** stereoisomeric forms, respectively, while Fig. 4 represents the matrices for all distance-angle pairs. Among the matrices with regard to the first subgroup of pharmacophores, five matrices (*i.e.*, (N-A) – (N-A-B), (N-A) – (N-B-A), (N-A) – (A-N-B), (N-B) – (N-B-A) and (A-B) – (N-B-A) matrices; see Figs. 4a-c, 4e and 4h) showed a very high similarity (*i.e.*, $0.95 \leq CS_{xx}$) in the case of **S[1]** – **S[2]** and **S[3]** – **S[4]** pairs. Based on these matrices, however, it could be concluded that lower similarity was detected for the four types of *cis* – *trans* stereoisomeric pairs (*i.e.*, **S[1]** – **S[3]**, **S[1]** – **S[4]**, **S[2]** – **S[3]** and **S[2]** – **S[4]** pairs), in comparison with those found for the *trans* – *trans* and *cis* – *cis* pairs. Taking into account these CS_{xx} indices, three different ranges could be distinguished - indicating high, moderate and low similarities, respectively -, as follows: (1) the first range (*i.e.*, 0.73-0.76) for the (N-A) – (N-B-A) matrix (see Fig. 4b); (2) the second range (*i.e.*, 0.49-0.62) for the

(N-A) – (N-A-B), (N-A) – (A-N-B) and (A-B) – (N-B-A) matrices (see Figs. 4a, 4c and 4h); (3) the third range (*i.e.*, 0.22-0.31) for the (N-B) – (N-B-A) matrix (see Fig. 4e). In the case of the other four matrices (*i.e.*, (N-B) – (N-A-B), (N-B) – (A-N-B), (A-B) – (N-A-B) and (A-B) – (A-N-B) matrices; see Figs. 4d, 4f, 4g and 4i) concerning the first subgroup, a high similarity (*i.e.*, $0.86 \leq CS_{xx} \leq 0.94$) was also observed for the **S[1]** – **S[2]** and **S[3]** – **S[4]** pairs. Nevertheless, these CS_{xx} indices were found to be slightly lower as compared to those detected for the five matrices. Additionally, larger differences were observed between the CS_{xx} indices calculated for the *trans* – *trans* and *cis* – *cis* pairs. Moreover, the above-mentioned four matrices indicate a very low similarity (*i.e.*, $0.07 \leq CS_{xx} \leq 0.19$) in the case of the four types of *cis* – *trans* stereoisomeric pairs.

The nine distance-angle plots, with regard to the second subgroup of pharmacophores, are displayed in Figs. 5 and 6 for the **S[3]** and **S[4]** stereoisomers, respectively, whereas Fig. 7 shows the matrices in the case of each distance-angle pair. Five matrices (*i.e.*,

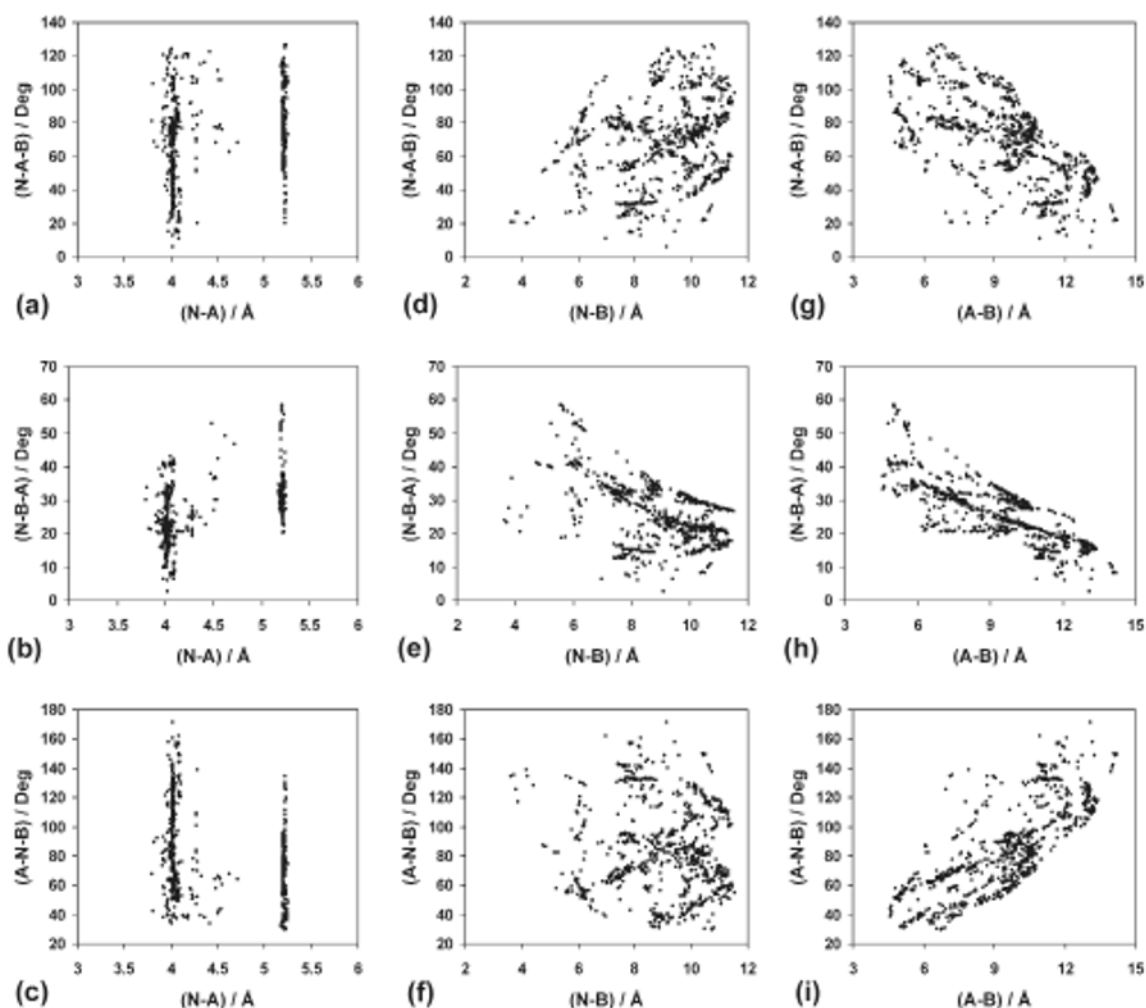


Figure 2. Nine different types of distance-angle maps, regarding the first subgroup of pharmacophore elements, for the **S[1]** stereoisomer: (a) the **(N-A) – (N-A-B)**, (b) the **(N-A) – (N-B-A)**, (c) the **(N-A) – (A-N-B)**, (d) the **(N-B) – (N-A-B)**, (e) the **(N-B) – (N-B-A)**, (f) the **(N-B) – (A-N-B)**, (g) the **(A-B) – (N-A-B)**, (h) the **(A-B) – (N-B-A)** and (i) the **(A-B) – (A-N-B)** plots.

(N-A) – (N-A-C), **(N-A) – (N-C-A)**, **(N-A) – (A-N-C)**, **(N-C) – (N-C-A)** and **(A-C) – (N-C-A)** matrices; see Figs. 7a-c, 7e and 7h) corresponding to the second subgroup of pharmacophore elements indicated a very high similarity (*i.e.*, $0.95 \leq CS_{xx}$) for the *trans – trans* and *cis – cis* stereoisomeric pairs. Nevertheless, these matrices show that lower similarity could be observed in the case of the four types of *cis – trans* pairs, as compared to those detected for the **S[1] – S[2]** and **S[3] – S[4]** stereoisomeric pairs. Among these five matrices, the **(N-A) – (N-C-A)** matrix revealed the higher similarity (*i.e.*, $0.85 \leq CS_{xx} \leq 0.92$; see Fig. 7b), whereas the **(N-C) – (N-C-A)** matrix showed the lower similarity (*i.e.*, $0.49 \leq CS_{xx} \leq 0.59$; see Fig. 7e), taking into account the four *cis – trans* pairs. For the other four matrices (*i.e.*, **(N-C) – (N-A-C)**, **(N-C) – (A-N-C)**, **(A-C) – (N-A-C)** and **(A-C) – (A-N-C)** matrices; see Figs. 7d, 7f, 7g and 7i)

corresponding to the second subgroup, a high similarity (*i.e.*, $0.73 \leq CS_{xx} \leq 0.85$) could also be found in the case of *trans – trans* and *cis – cis* stereoisomeric pairs. Considering these CS_{xx} indices, it could be concluded that on the one hand, they proved to be lower compared to those found for the five matrices, and on the other hand, their differences were found to be larger with regard to the **S[1] – S[2]** and **S[3] – S[4]** pairs. On the basis of four matrices, however, it could be deduced that a low similarity (*i.e.*, $0.21 \leq CS_{xx} \leq 0.37$) could be detected for the four types of *cis – trans* pairs.

As the aforementioned results indicate, similar observations could be made for the two subgroups of pharmacophore elements, based on the comparative analysis of various conformational distributions concerning the four stereoisomers of tetrapeptide. In the case of both subgroups of pharmacophores, the nine

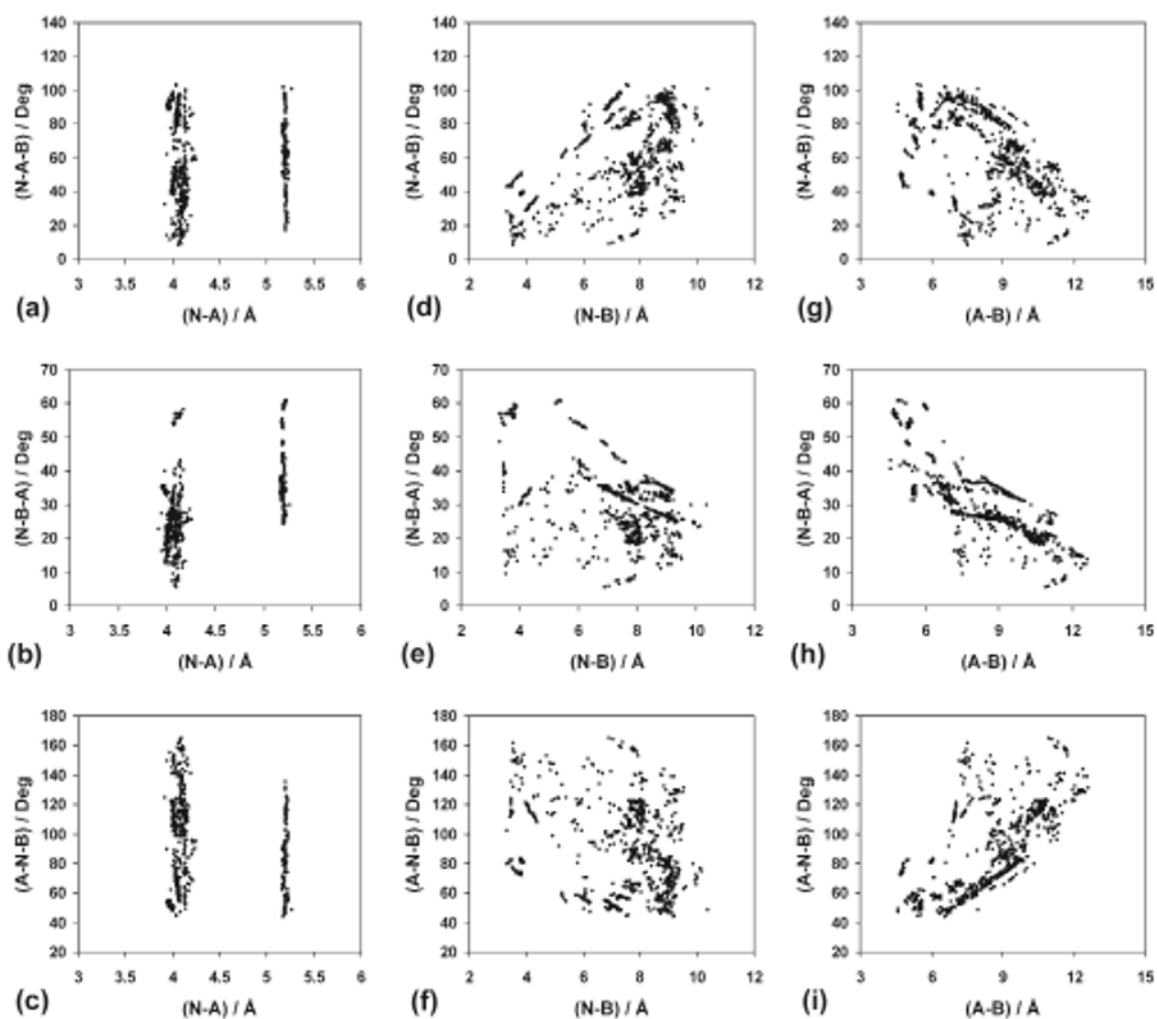


Figure 3. Nine different types of distance-angle maps, regarding the first subgroup of pharmacophore elements, for the **S[2]** stereoisomer: (a) the **(N-A) – (N-A-B)**, (b) the **(N-A) – (N-B-A)**, (c) the **(N-A) – (A-N-B)**, (d) the **(N-B) – (N-B-A)**, (e) the **(N-B) – (N-B-A)**, (f) the **(N-B) – (A-N-B)**, (g) the **(A-B) – (N-A-B)**, (h) the **(A-B) – (N-B-A)** and (i) the **(A-B) – (A-N-B)** plots.

matrices could be divided into two different classes, as follows: (1) the first class covered five types of matrices (*i.e.*, **(N-A) – (N-A-B/C)**, **(N-A) – (N-B/C-A)**, **(N-A) – (A-N-B/C)**, **(N-B/C) – (N-B/C-A)** and **(A-B/C) – (N-B/C-A)** matrices); (2) the second class included four types of matrices (*i.e.*, **(N-B/C) – (N-A-B/C)**, **(N-B/C) – (A-N-B/C)**, **(A-B/C) – (N-A-B/C)** and **(A-B/C) – (A-N-B/C)** matrices). Taking into account the first class of matrices, it could be concluded that approximately the same CS_{xx} index was detected regarding the *trans – trans* and *cis – cis* pairs for both subgroups of pharmacophores, whereas the CS_{xx} indices calculated for the four *cis – trans* pairs were found to be larger in the case of second subgroup than those observed for the first one. The matrices belonging to the second class indicate that for the second subgroup of pharmacophore elements,

the CS_{xx} indices concerning the *trans – trans* and *cis – cis* pairs proved to be smaller, while the CS_{xx} indices regarding the *cis – trans* pairs proved to be larger, as compared to those detected in the case of first subgroup. Based on the distance-angle maps pertaining to the first class of matrices, the **S[1]** and **S[2]**, as well as the **S[3]** and **S[4]** stereoisomeric pairs can be slightly separated from each other. Nevertheless, distinctions can be made with regard to the **S[1] – S[3]**, **S[1] – S[4]**, **S[2] – S[3]** and **S[2] – S[4]** pairs. Considering the distance-angle plots belonging to the second class of matrices, a similar conclusion could be made for the four *cis – trans* pairs; however, on the basis of these plots, it was possible to differentiate between the *trans* isomer pairs, as well as between the *cis* isomer pairs, regarding the parent peptide and its *enanti*o form.

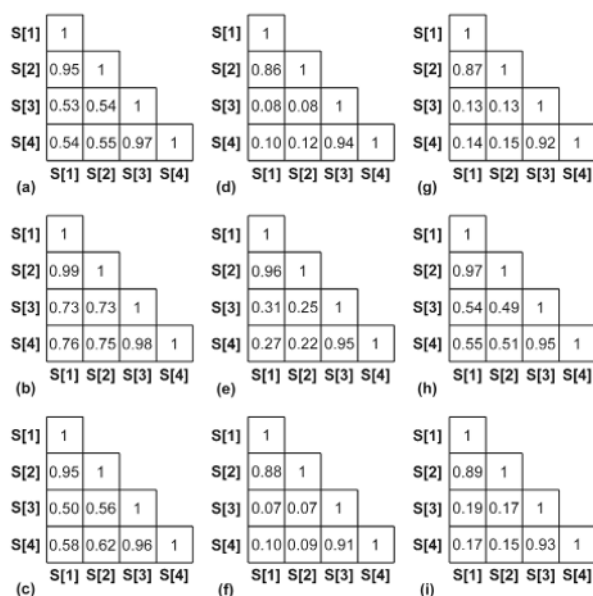


Figure 4. Nine matrices concerning the first subgroup of pharmacophores: (a) the (N-A) – (N-A-B), (b) the (N-A) – (N-B-A), (c) the (N-A) – (A-N-B), (d) the (N-B) – (N-A-B), (e) the (N-B) – (N-B-A), (f) the (N-B) – (A-N-B), (g) the (A-B) – (N-A-B), (h) the (A-B) – (N-B-A) and (i) the (A-B) – (A-N-B) matrices.

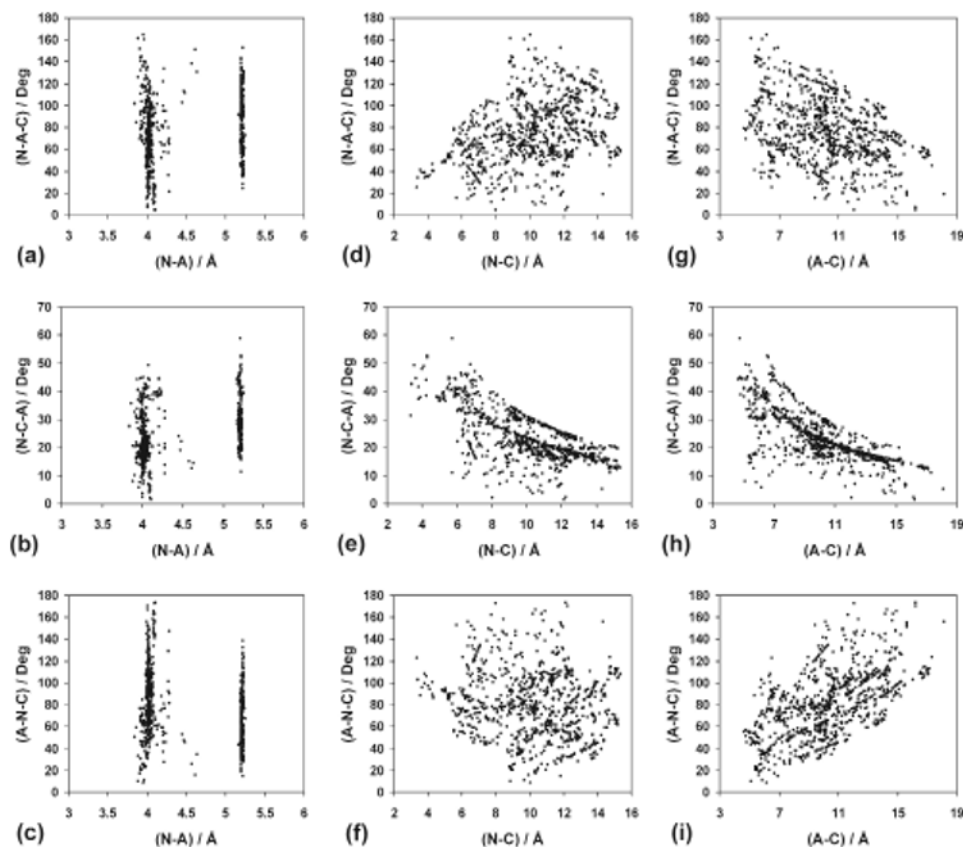


Figure 5. Nine different types of distance-angle maps, regarding the second subgroup of pharmacophore elements, for the S[3] stereoisomer: (a) the (N-A) – (N-A-C), (b) the (N-A) – (N-C-A), (c) the (N-A) – (A-N-C), (d) the (N-C) – (N-A-C), (e) the (N-C) – (N-C-A), (f) the (N-C) – (A-N-C), (g) the (A-C) – (N-A-C), (h) the (A-C) – (N-C-A) and (i) the (A-C) – (A-N-C) plots.

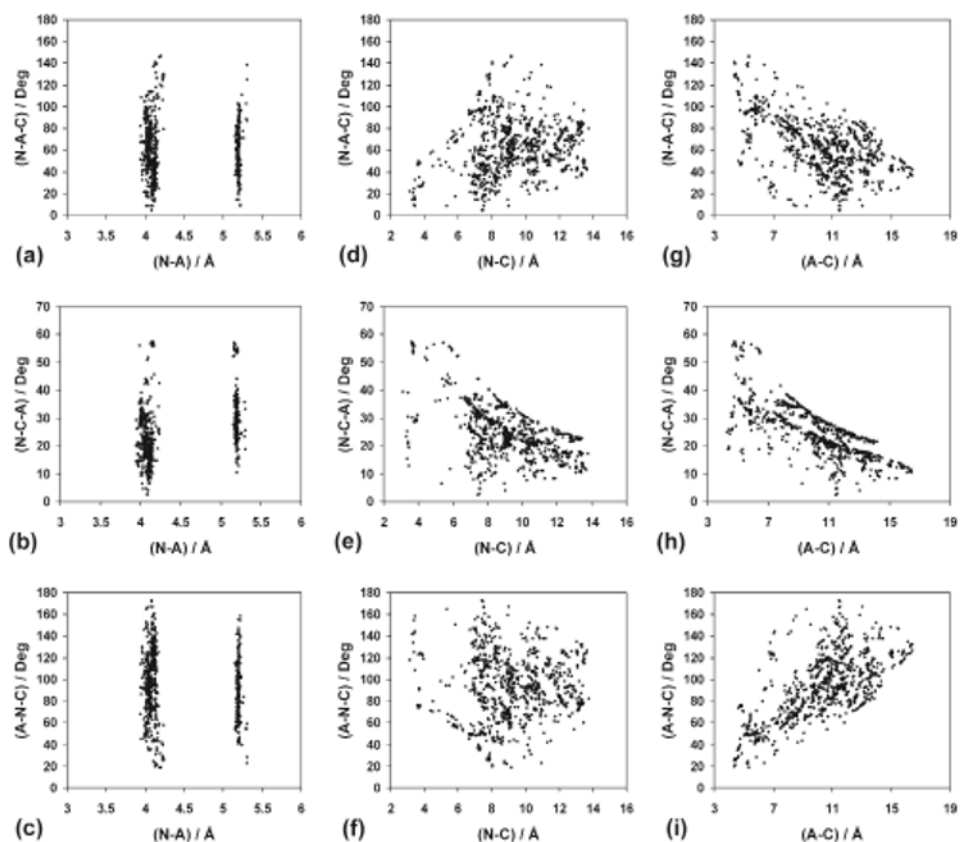


Figure 6. Nine different types of distance-angle maps, regarding the second subgroup of pharmacophore elements, for the **S[4]** stereoisomer: (a) the (N-A) – (N-A-C), (b) the (N-A) – (N-C-A), (c) the (N-A) – (A-N-C), (d) the (N-C) – (N-A-C), (e) the (N-C) – (N-C-A), (f) the (N-C) – (A-N-C), (g) the (A-C) – (N-A-C), (h) the (A-C) – (N-C-A) and (i) the (A-C) – (A-N-C) plots.

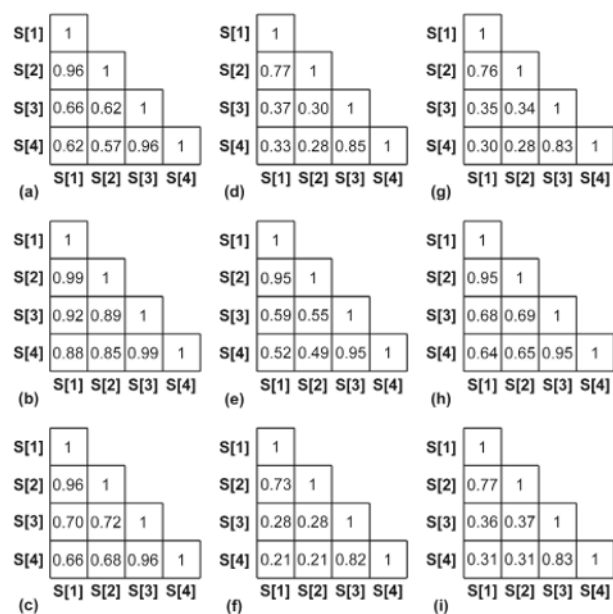


Figure 7. Nine matrices concerning the second subgroup of pharmacophores: (a) the (N-A) – (N-A-C), (b) the (N-A) – (N-C-A), (c) the (N-A) – (A-N-C), (d) the (N-C) – (N-A-C), (e) the (N-C) – (N-C-A), (f) the (N-C) – (A-N-C), (g) the (A-C) – (N-A-C), (h) the (A-C) – (N-C-A) and (i) the (A-C) – (A-N-C) matrices.

4. Conclusions

All the results obtained by the present theoretical study suggest that the stereoisomeric forms of EM2 could be discriminated from one another based on the comparative analysis of conformational distributions concerning the pharmacophore elements of the tetrapeptide. Taking into account each distance-angle pair, it could be deduced that to distinguish between the stereoisomers, the distance-angle maps pertaining to the second class of matrices proved to be more suitable than the first class of matrices. Moreover, the distance-angle maps regarding the first subgroup of pharmacophores seemed to be more appropriate in the majority of cases, to differentiate between the stereoisomeric forms, as compared to those concerning the second subgroup of pharmacophores. Nevertheless, the comparative analysis led to the observation that certain geometric parameters could be considered as least discriminatory parameters, as compared to the others, namely, the (**N-A**) distance for both subgroups of

pharmacophores, as well as the (**N-B-A**) and (**N-C-A**) angles for the first and second subgroups, respectively. On the whole, it could be concluded that the various distance-angle maps, as well as the CSP approach could be also applied in the case of the stereoisomeric forms of the tetrapeptide, in order to distinguish them from one another. This conclusion indicates that the comparative analysis of various conformational distributions, regarding the pharmacophore elements of the stereoisomers, would be useful to investigate the effects of both L-D and *cis-trans* isomerisms on the spatial relationships of the pharmacophores of peptides.

Acknowledgements

This research was supported by the Hungarian Scientific Research Fund (OTKA PD 78554), and by the János Bolyai Research Scholarship of the Hungarian Academy of Sciences.

References

- [1] J.E. Zadina, L. Hackler, L.-J. Ge, A.J. Kastin, *Nature* 386, 499 (1997)
- [2] B. Leitgeb, *Chem. Biodiv.* 4, 2703 (2007)
- [3] B. Leitgeb, F. Ötvös, G. Tóth, *Biopolymers* 68, 497 (2003)
- [4] B. Leitgeb, A. Szekeres, G. Tóth, *J. Pept. Res.* 62, 145 (2003)
- [5] B. Leitgeb, A. Szekeres, *J. Mol. Struct. – THEOCHEM* 666-667, 337 (2003)
- [6] B. Leitgeb, G. Tóth, *Eur. J. Med. Chem.* 40, 674 (2005)
- [7] B. Leitgeb, *Chem. Biol. Drug Des.* 79, 313 (2012)
- [8] D. Bernard, A. Coop, A.D. MacKerell Jr, *J. Am. Chem. Soc.* 125, 3101 (2003)
- [9] D. Bernard, A. Coop, A.D. MacKerell Jr, *J. Med. Chem.* 48, 7773 (2005)
- [10] D. Bernard, A. Coop, A.D. MacKerell Jr, *J. Med. Chem.* 50, 1799 (2007)
- [11] D.A. Case, T.A. Darden, T.E. Cheatham III, C.L. Simmerling, J. Wang, R.E. Duke, R. Luo, K.M. Merz, D.A. Pearlman, M. Crowley, R.C. Walker, W. Zhang, B. Wang, S. Hayik, A. Roitberg, G. Seabra, K.F. Wong, F. Paesani, X. Wu, S. Brozell, V. Tsui, H. Gohlke, L. Yang, C. Tan, J. Mongan, V. Hornak, G. Cui, P. Beroza, D.H. Mathews, C. Schafmeister, W.S. Ross, P.A. Kollman, *AMBER 9* (University of California, San Francisco, 2006)
- [12] V. Hornak, R. Abel, A. Okur, B. Strockbine, A. Roitberg, C. Simmerling, *Proteins* 65, 712 (2006)
- [13] G.D. Hawkins, C.J. Cramer, D.G. Truhlar, *Chem. Phys. Lett.* 246, 122 (1995)
- [14] G.D. Hawkins, C.J. Cramer, D.G. Truhlar, *J. Phys. Chem.* 100, 19824 (1996)
- [15] V. Tsui, D.A. Case, *Biopolymers (Nucl. Acid Sci.)* 56, 275 (2001)
- [16] D. Pal, P. Chakrabarti, *J. Biomol. Struct. Dyn.* 18, 273 (2000)
- [17] P. Chakrabarti, D. Pal, *Prog. Biophys. Mol. Biol.* 76, 1 (2001)